

# Site-Selective Internal Cross-Linking between Mercury(II)-Centered Vertices of an Octahedral Mercury(II) Capsule by a Rod-Shaped Ditopic Ligand\*\*

Shuichi Hiraoka,\* Madoka Kiyokawa, Shizuka Hashida, and Mitsuhiro Shionoya\*

Artificial molecular capsules,<sup>[1–6]</sup> which can provide a well-defined nanosized space, have been used extensively for highly specific molecular recognition and reactions.<sup>[7]</sup> For such nanospaces to be exploited for a variety of purposes, it is essential that they can be partitioned or chemically modified by predefined functional groups. However, in self-assembly processes, such modifications have been made by the use of chemically premodified building blocks in the one-step construction of the entity, because it is rather hard in general to decorate the interior of three-dimensional capsule structures with control of the arrangement of functional groups after the initial self-assembly process.<sup>[8]</sup> Since the inner space is isolated and protected by the shell of the capsule, the access of chemical species to the interior should be kinetically unfavorable. Therefore, when such compounds can react at both the inner and the outer surfaces of the capsule shell, the outer surface should be functionalized preferentially. In particular, when a self-assembled molecular capsule is formed through H bonding<sup>[2]</sup> and/or metal coordination,<sup>[3,4]</sup> the capsule structure tends to collapse under harsh conditions owing to its lability. Furthermore, the addition of other components to the capsules may displace the equilibrium to generate alternative structures. Thus, a facile method for interior chemical modification under mild conditions is vital to the development of self-assembled molecular capsules.

Recently, we reported the quantitative formation of octahedron-shaped metallocapsules,  $[M_6\mathbf{1}_8]^{12+}$ , from ten kinds of divalent transition-metal ions (M: Mn, Fe, Co, Ni, Cu, Pd, Pt, Zn, Cd, and Hg).<sup>[4c]</sup> Single-crystal X-ray analysis and <sup>19</sup>F NMR spectroscopy of the  $[\text{Hg}_6\mathbf{1}_8(\text{OTf})_{12}]$  capsule revealed that each Hg<sup>II</sup> ion at a vertex is bound by four pyridyl

nitrogen atoms and two TfO<sup>−</sup> axial ligands from the inside and outside of the capsule to form an octahedral six-coordinate geometry (Figure 1). Furthermore, we found that these six inner TfO<sup>−</sup> ligands (TfO<sub>in</sub><sup>−</sup>) can be replaced site selectively by other sulfonate ligands.<sup>[4c]</sup> Therefore, this site-selective ligand exchange could become useful for functionalization of the inner wall of the precursor capsule,  $[\text{M}_6\mathbf{1}_8 \cdot (\text{TfO}_{\text{in}})_6 \cdot (\text{TfO}_{\text{out}})_6]$ , with various sulfonate ligands. If it is possible to site selectively introduce and arrange functional groups at the core of the capsule, both the core and the inner walls in the confined space of the nanocapsules could be

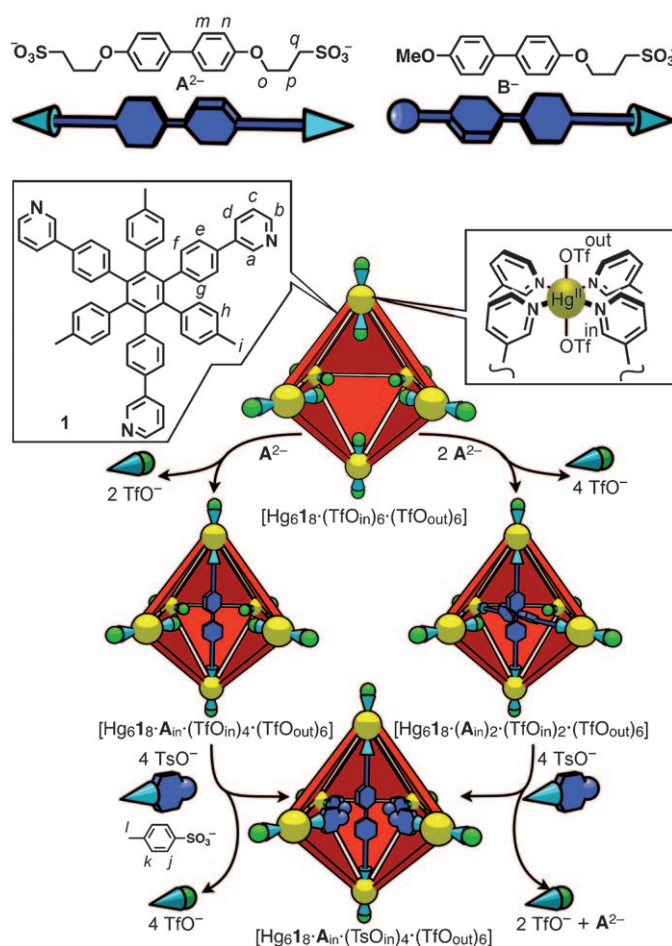


**Figure 1.** Schematic representation of site-selective ligand exchange in the octahedral Hg<sup>II</sup> capsule with ditopic bridging ligand(s) **A<sup>2−</sup>**. The two front ligands **1** of the  $[\text{Hg}_6\mathbf{1}_8(\text{TfO}_{\text{in}})_6(\text{TfO}_{\text{out}})_6]$  capsule are omitted to enable the interior of the capsule to be seen. Tf = trifluoromethanesulfonyl, Ts = *p*-toluenesulfonyl.

[\*] Dr. S. Hiraoka, M. Kiyokawa, S. Hashida, Prof. Dr. M. Shionoya  
Department of Chemistry, Graduate School of Science  
The University of Tokyo  
7-3-1 Hongo, Bunkyo-ku, Tokyo 113-0033 (Japan)  
Fax: (+81) 3-5841-8061  
E-mail: hiraoka@chem.s.u-tokyo.ac.jp  
shionoya@chem.s.u-tokyo.ac.jp

Dr. S. Hiraoka  
Precursory Research for Embryonic Science and Technology  
(PRESTO), Japan Science and Technology Agency  
4-1-8 Honcho, Kawaguchi, Saitama 332-0012 (Japan)  
Fax: (+81) 3-5841-1530

[\*\*] This research is supported by Grants-in-Aid from MEXT of Japan and the Global COE Program for Chemistry Innovation.

Supporting information for this article, including details of the experimental procedures, is available on the WWW under <http://dx.doi.org/10.1002/anie.200905449>.

decorated elaborately to form an isolated functional nanospace. A promising strategy towards this goal would be to bridge the two metal centers at the opposite vertices of the octahedral capsule with a ditopic bisulfonate bridging ligand, whereby the center of the bisulfonate ligand should be set around the core of the capsule.

On the basis of the crystal structure of the  $[\text{Hg}_6\mathbf{1}_8\text{-(TfO}_{\text{in}})_6\text{-(TfO}_{\text{out}})_6}]$  capsule, in which  $\text{Hg}^{\text{II}}$  centers at opposite vertices are located 2.5 nm apart, we have designed a rod-shaped bisulfonate  $\mathbf{A}^{2-}$  as a ditopic bridging ligand (Figure 1). The distance between the two anionic oxygen atoms of  $\mathbf{A}^{2-}$  was estimated to be approximately 2.0 nm; therefore, we believed that  $\mathbf{A}^{2-}$  would be an appropriate molecule for bridging two  $\text{Hg}^{\text{II}}$  centers.<sup>[4c]</sup> Herein, we describe the site-selective replacement of  $\text{TfO}_{\text{in}}^-$  in the  $[\text{Hg}_6\mathbf{1}_8\text{-(TfO}_{\text{in}})_6\text{-(TfO}_{\text{out}})_6}]$  capsule with  $\mathbf{A}^{2-}$ , which can bridge two  $\text{Hg}^{\text{II}}$  centers at opposite vertices of the octahedral capsule to selectively form  $[\text{Hg}_6\mathbf{1}_8\text{-(A}_{\text{in}})_2\text{-(TfO}_{\text{in}})_4\text{-(TfO}_{\text{out}})_6}]$  and  $[\text{Hg}_6\mathbf{1}_8\text{-(A}_{\text{in}})_2\text{-(TfO}_{\text{in}})_2\text{-(TfO}_{\text{out}})_6}]$ . This method also enables the site-selective introduction of two different sulfonate ligands,  $\mathbf{A}^{2-}$  and a benzenesulfonate ( $\text{TsO}^-$  or *p*-chlorobenzenesulfonate), into the capsule. Thus, the 2 nm wide inner space of the  $\text{Hg}^{\text{II}}$  capsule can be decorated in a highly controllable manner.

The site-selective ligand exchange of the inner  $\text{TfO}_{\text{in}}^-$  ligands of the capsule  $[\text{Hg}_6\mathbf{1}_8\text{-(TfO}_{\text{in}})_6\text{-(TfO}_{\text{out}})_6}]$  in  $\text{CD}_3\text{CN}$  was monitored by  $^1\text{H}$  and  $^{19}\text{F}$  NMR spectroscopy and electrospray ionization-time-of-flight (ESI-TOF) mass spectrometry. The  $^{19}\text{F}$  NMR spectrum of the capsule in  $\text{CD}_3\text{CN}$  showed two signals at  $\delta = 86.1$  and  $85.2$  ppm ( $\text{C}_6\text{F}_6$ :  $\delta = 0$  ppm), which were assigned to the inner  $\text{TfO}_{\text{in}}^-$  and outer  $\text{TfO}_{\text{out}}^-$  ligands, respectively (see Figure S1A in the Supporting Information).<sup>[9]</sup> When  $\text{Me}_4\text{NOTs}$  (6 equiv) was added to a solution of  $[\text{Hg}_6\mathbf{1}_8\text{-(TfO}_{\text{in}})_6\text{-(TfO}_{\text{out}})_6}]$  in  $\text{CD}_3\text{CN}$ , the  $^{19}\text{F}$  NMR signal assigned to  $\text{TfO}_{\text{in}}^-$  disappeared, and only a signal for  $\text{TfO}_{\text{out}}^-$  was observed (see Figure S1B in the Supporting Information). This result suggests that  $[\text{Hg}_6\mathbf{1}_8\text{-(TsO}_{\text{in}})_6\text{-(TfO}_{\text{out}})_6}]$  is formed by the site-selective replacement of the six  $\text{TfO}_{\text{in}}^-$  ligands with six  $\text{TsO}^-$  ligands. This ligand exchange was also confirmed by the  $^1\text{H}$  NMR spectrum, in which the signals for  $\text{TsO}_{\text{in}}^-$  were shifted downfield relative to those for  $\text{Me}_4\text{NOTs}$  (Figures 3B,C). Furthermore, the signal of one of the pyridyl hydrogen atoms located inside the capsule,  $\text{H}^a$ , was shifted downfield, whereas no significant change was observed in the chemical-shift value of that of the outer pyridyl hydrogen atom,  $\text{H}^b$ . This result also indicates the site-selective ligand exchange of inner  $\text{TfO}_{\text{in}}^-$ .

The ESI-TOF mass spectrum of  $[\text{Hg}_6\mathbf{1}_8\text{-(TfO}_{\text{in}})_6\text{-(TfO}_{\text{out}})_6}]$  showed a prominent signal for a cationic species  $[\text{Hg}_6\mathbf{1}_8\text{-(TfO)}_n]^{(12-n)+}$  ( $n = 6-8$ ) as well as a considerably weaker signal for  $[\text{Hg}_6\mathbf{1}_8\text{-(TfO)}_5]^{7+}$  (see Figure S2A in the Supporting Information). These results suggest that the outer six  $\text{TfO}_{\text{out}}^-$  ligands can be removed more easily than the inner  $\text{TfO}_{\text{in}}^-$  ligands from the  $[\text{Hg}_6\mathbf{1}_8\text{-(TfO}_{\text{in}})_6\text{-(TfO}_{\text{out}})_6}]$  capsule during the ionization process, and therefore that the septuply charged species lacking one  $\text{TfO}_{\text{in}}^-$  ligand,  $[\text{Hg}_6\mathbf{1}_8\text{-(TfO)}_5]^{7+}$ , should be hard to generate. Indeed, the ESI-TOF mass spectrum of  $[\text{Hg}_6\mathbf{1}_8\text{-(TsO}_{\text{in}})_6\text{-(TfO}_{\text{out}})_6}]$  exhibited prominent signals for  $[\text{Hg}_6\mathbf{1}_8\text{-(TsO)}_n\text{-(TfO)}_n]^{6-n}$  ( $n = 0-2$ ) with six  $\text{TsO}^-$  ligands (see Figure S2B in the Supporting Information); that

is, no signals were observed for species lacking a  $\text{TsO}^-$  ligand. On the basis of these findings, we further investigated the ligand exchange of  $\text{TfO}_{\text{in}}^-$  with a sulfonate ligand,  $\mathbf{A}^{2-}$ , by NMR spectroscopy and ESI-TOF mass spectrometry.

Upon the addition of  $\mathbf{A}\cdot(n\text{Bu}_4\text{N})_2$  to a solution of  $[\text{Hg}_6\mathbf{1}_8\text{-(TfO}_{\text{in}})_6\text{-(TfO}_{\text{out}})_6}]$  in  $\text{CD}_3\text{CN}$ , the intensity of the  $^{19}\text{F}$  NMR signal assigned to  $\text{TfO}_{\text{in}}^-$  decreased until 2 equivalents of  $\mathbf{A}^{2-}$  relative to the capsule had been added (Figure 2). Although the addition of more than 2 equivalents of  $\mathbf{A}\cdot(n\text{Bu}_4\text{N})_2$

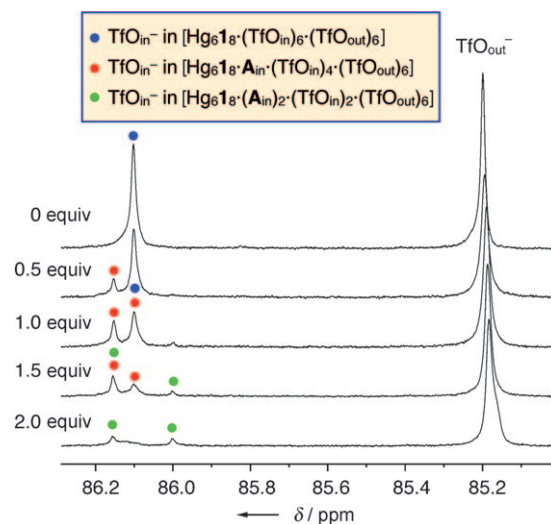


**Figure 2.** Titrimetric  $^{19}\text{F}$  NMR spectra of  $[\text{Hg}_6\mathbf{1}_8\text{-(TfO}_{\text{in}})_6\text{-(TfO}_{\text{out}})_6}]$  with  $\mathbf{A}\cdot(n\text{Bu}_4\text{N})_2$  (0–2 equiv; 470 MHz,  $\text{CD}_3\text{CN}$ , 263 K;  $\text{C}_6\text{F}_6$  ( $\delta = 0$  ppm) was used as the internal standard).

resulted in the formation of a precipitate, the signal for  $\text{TfO}_{\text{in}}^-$  still remained. This result indicates that up to four  $\text{TfO}_{\text{in}}^-$  ligands can be replaced with two  $\mathbf{A}^{2-}$  ligands, and that the ligand exchange of  $\text{TfO}_{\text{out}}^-$  with  $\mathbf{A}^{2-}$  in the presence of more than 2 equivalents of  $\mathbf{A}\cdot(n\text{Bu}_4\text{N})_2$  produces poorly soluble compounds.

A titrimetric ESI-TOF mass spectrometric study revealed that the ligand exchange of  $\text{TfO}_{\text{in}}^-$  with  $\mathbf{A}^{2-}$  took place in a nearly stepwise manner. Upon the addition of 1 equivalent of  $\mathbf{A}\cdot(n\text{Bu}_4\text{N})_2$  to a solution of  $[\text{Hg}_6\mathbf{1}_8\text{-(TfO}_{\text{in}})_6\text{-(TfO}_{\text{out}})_6}]$  in  $\text{CD}_3\text{CN}$ ,<sup>[10]</sup> signals assignable to  $[\text{Hg}_6\mathbf{1}_8\text{·A}_{\text{in}}\text{·(TfO}_{\text{in}})_4]^{6+}$  were observed (see Figure S3C in the Supporting Information). When excess  $\mathbf{A}^{2-}$  was added, the complex  $[\text{Hg}_6\mathbf{1}_8\text{·(A}_{\text{in}})_2\text{·(TfO}_{\text{in}})_2\text{·(TfO}_{\text{out}})_6}]$  was then formed selectively (see Figure S3D in the Supporting Information). The addition of more than 2 equivalents of  $\mathbf{A}^{2-}$  did not lead to any change in the spectrum, although the intensity of the signals decreased as a result of precipitation (see Figure S5 in the Supporting Information). These results clearly indicate that the two  $\text{TfO}_{\text{in}}^-$  ligands can be replaced with one  $\mathbf{A}^{2-}$  ligand to form two substituted species,  $[\text{Hg}_6\mathbf{1}_8\text{·A}_{\text{in}}\text{·(TfO}_{\text{in}})_4\text{·(TfO}_{\text{out}})_6}]$  and  $[\text{Hg}_6\mathbf{1}_8\text{·(A}_{\text{in}})_2\text{·(TfO}_{\text{in}})_2\text{·(TfO}_{\text{out}})_6}]$ , in a stepwise manner.<sup>[11]</sup>

Upon the addition of  $\mathbf{A}\cdot(n\text{Bu}_4\text{N})_2$  (1 equiv) to a solution of  $[\text{Hg}_6\mathbf{1}_8\text{-(TfO}_{\text{in}})_6\text{-(TfO}_{\text{out}})_6}]$  in  $\text{CD}_3\text{CN}$  in the titrimetric  $^1\text{H}$  NMR study, several  $^1\text{H}$  signals for  $[\text{Hg}_6\mathbf{1}_8\text{·A}_{\text{in}}\text{·(TfO}_{\text{in}})_4\text{·(TfO}_{\text{out}})_6}]$  appeared in addition to those for  $[\text{Hg}_6\mathbf{1}_8\text{-(TfO}_{\text{in}})_6\text{·(TfO}_{\text{out}})_6}]$  (Figure 3D). This result indicates that the forma-

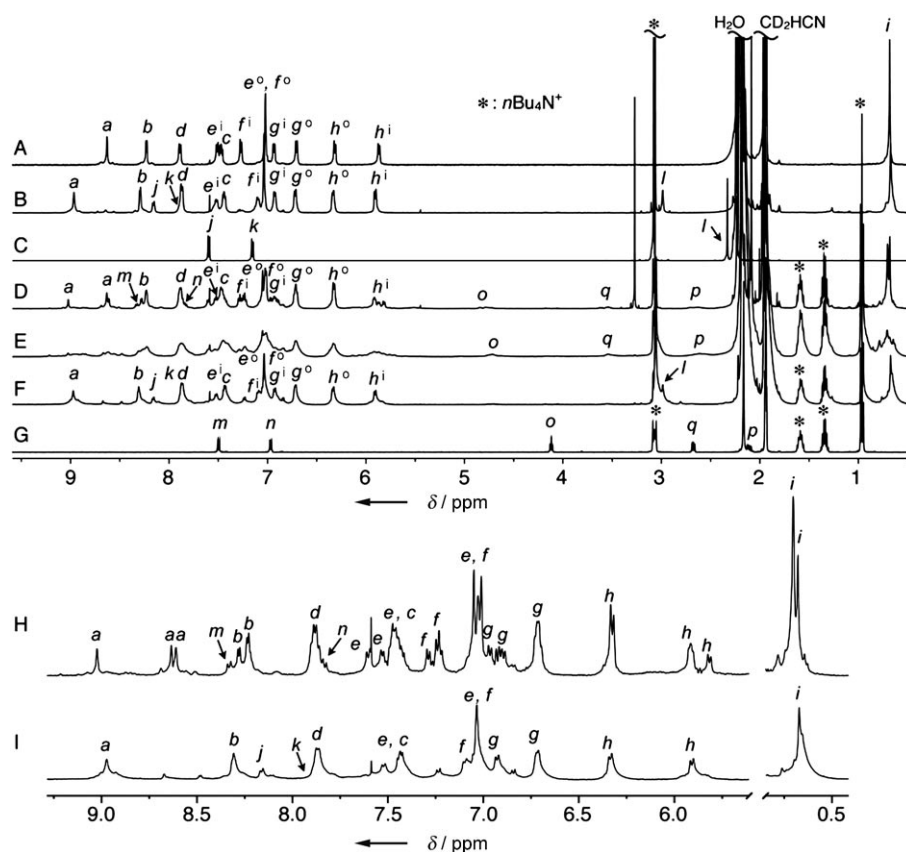


**Figure 3.**  $^1\text{H}$  NMR spectra (500 MHz,  $\text{CD}_3\text{CN}$ , 293 K,  $[\text{Hg}_6\mathbf{1}_8] = 0.27 \text{ mM}$ ): A)  $[\text{Hg}_6\mathbf{1}_8 \cdot (\text{TfO}_{\text{in}})_6 \cdot (\text{TfO}_{\text{out}})_6]$ ; B)  $[\text{Hg}_6\mathbf{1}_8 \cdot (\text{TsO}_{\text{in}})_6 \cdot (\text{TfO}_{\text{out}})_6]$ ; C)  $\text{Me}_4\text{NOTs}$ ; D)  $[\text{Hg}_6\mathbf{1}_8 \cdot (\text{TfO}_{\text{in}})_6 \cdot (\text{TfO}_{\text{out}})_6]$  with  $\text{A} \cdot (\text{nBu}_4\text{N})_2$  (1 equiv), which provides a mixture of  $[\text{Hg}_6\mathbf{1}_8 \cdot (\text{TfO}_{\text{in}})_6 \cdot (\text{TfO}_{\text{out}})_6]$  and  $[\text{Hg}_6\mathbf{1}_8 \cdot \text{A}_{\text{in}} \cdot (\text{TfO}_{\text{in}})_4 \cdot (\text{TfO}_{\text{out}})_6]$ ; E)  $[\text{Hg}_6\mathbf{1}_8 \cdot (\text{TfO}_{\text{in}})_6 \cdot (\text{TfO}_{\text{out}})_6]$  with  $\text{A} \cdot (\text{nBu}_4\text{N})_2$  (2 equiv); F)  $[\text{Hg}_6\mathbf{1}_8 \cdot \text{A}_{\text{in}} \cdot (\text{TsO}_{\text{in}})_4 \cdot (\text{TfO}_{\text{out}})_6]$  prepared from the solution in (E) with  $\text{Me}_4\text{NOTs}$  (4 equiv); G)  $\text{A} \cdot (\text{nBu}_4\text{N})_2$ ; H) difference  $^1\text{H}$  NMR spectrum obtained by subtracting (A) from (D) to discriminate the signals of  $[\text{Hg}_6\mathbf{1}_8 \cdot \text{A}_{\text{in}} \cdot (\text{TfO}_{\text{in}})_4 \cdot (\text{TfO}_{\text{out}})_6]$  from the other signals; I) magnified view of the aromatic region and *p*-tolyl signals in (F). The symbols  $e^i$ ,  $f$ ,  $g$ , and  $h^i$ , and  $e^\circ$ ,  $f^\circ$ ,  $g^\circ$ , and  $h^\circ$  denote the signals of chemically nonequivalent inner and outer phenylene hydrogen atoms of the capsule, respectively.

tion of  $[\text{Hg}_6\mathbf{1}_8 \cdot \text{A}_{\text{in}} \cdot (\text{TfO}_{\text{in}})_4 \cdot (\text{TfO}_{\text{out}})_6]$  is not quantitative, as was also confirmed by ESI-TOF mass spectrometry (see Figure S3C in the Supporting Information). It appears from the peak integrals that  $[\text{Hg}_6\mathbf{1}_8 \cdot \text{A}_{\text{in}} \cdot (\text{TfO}_{\text{in}})_4 \cdot (\text{TfO}_{\text{out}})_6]$  and  $[\text{Hg}_6\mathbf{1}_8 \cdot (\text{TfO}_{\text{in}})_6 \cdot (\text{TfO}_{\text{out}})_6]$  coexist in the solution in a 8.8:1 ratio. To distinguish the signals of  $[\text{Hg}_6\mathbf{1}_8 \cdot \text{A}_{\text{in}} \cdot (\text{TfO}_{\text{in}})_4 \cdot (\text{TfO}_{\text{out}})_6]$  from those of  $[\text{Hg}_6\mathbf{1}_8 \cdot (\text{TfO}_{\text{in}})_6 \cdot (\text{TfO}_{\text{out}})_6]$ , a difference spectrum was prepared by subtracting the spectrum of  $[\text{Hg}_6\mathbf{1}_8 \cdot (\text{TfO}_{\text{in}})_6 \cdot (\text{TfO}_{\text{out}})_6]$  (Figure 3A) from that of the mixture of  $[\text{Hg}_6\mathbf{1}_8 \cdot \text{A}_{\text{in}} \cdot (\text{TfO}_{\text{in}})_4 \cdot (\text{TfO}_{\text{out}})_6]$  and  $[\text{Hg}_6\mathbf{1}_8 \cdot (\text{TfO}_{\text{in}})_6 \cdot (\text{TfO}_{\text{out}})_6]$  (Figure 3D). The resulting spectrum showed that all hydrogen atoms of **1** in  $[\text{Hg}_6\mathbf{1}_8 \cdot \text{A}_{\text{in}} \cdot (\text{TfO}_{\text{in}})_4 \cdot (\text{TfO}_{\text{out}})_6]$  were nonequivalent. For example, three  $\text{H}^a$  signals were observed with the same integral ratio. One of the three  $\text{H}^a$  hydrogen atoms showed a signal at  $\delta = 9.03 \text{ ppm}$  resulting from a downfield shift, whereas the remaining two hydrogen atoms exhibited signals at  $\delta = 8.63$  and  $8.61 \text{ ppm}$  with only a slight change in their chemical-shift values. Accordingly, the resonances at a lower magnetic field should be attributed to  $\text{H}^a$  hydrogen atoms of the pyridine rings coordinated to  $\text{Hg}^{\text{II}}$  bound by  $\text{A}^{2-}$ . No changes were observed in the chemical-

shift values of the signals for hydrogen atoms  $\text{H}^b$  located outside the capsule, on the other hand, which indicates that one  $\text{A}^{2-}$  ligand was introduced inside the capsule. The signals for the phenylene hydrogen atoms of  $\text{A}^{2-}$  in  $[\text{Hg}_6\mathbf{1}_8 \cdot \text{A}_{\text{in}} \cdot (\text{TfO}_{\text{in}})_4 \cdot (\text{TfO}_{\text{out}})_6]$ ,  $\text{H}^m$  and  $\text{H}^n$ , were observed at  $\delta = 8.33$  and  $7.83 \text{ ppm}$ , respectively, in the  $^1\text{H}$ - $^1\text{H}$  COSY spectrum (see Figure S9 in the Supporting Information). The  $^1\text{H}$  DOSY spectrum revealed the same  $\log D$  value of  $-9.2$  for the hydrogen atoms of both **1** and  $\text{A}^{2-}$  (see Figure S11 in the Supporting Information). This result also supports the incorporation of  $\text{A}^{2-}$  inside the capsule.<sup>[12]</sup>

Since  $\text{A}^{2-}$  is conformationally flexible, two different types of bridging are possible, as shown schematically in Figures 4A,B. We carried out  $^1\text{H}$  and  $^{19}\text{F}$  NMR spectroscopic studies to investigate the structure of the resulting capsules in detail (Figures 2 and 3).  $^1\text{H}$ - $^1\text{H}$  COSY and NOESY measurements (see Figures S9 and S10 in the Supporting Information) clearly indicated that when the  $[\text{Hg}_6\mathbf{1}_8 \cdot \text{A}_{\text{in}} \cdot (\text{TfO}_{\text{in}})_4 \cdot (\text{TfO}_{\text{out}})_6]$  capsule was formed, each  $^1\text{H}$  NMR signal of **1** for the original  $[\text{Hg}_6\mathbf{1}_8 \cdot (\text{TfO}_{\text{in}})_6 \cdot (\text{TfO}_{\text{out}})_6]$  capsule was divided into three signals with a 1:1:1 integral ratio. If a bisulfonate  $\text{A}^{2-}$  connects two adjacent  $\text{Hg}^{\text{II}}$  centers (Figure 4A), seven nonequivalent  $\text{H}^a$  signals should appear as a result of the  $C_{2v}$  symmetry of the resulting capsule. If  $\text{A}^{2-}$  bridges two opposite  $\text{Hg}^{\text{II}}$  vertices (Figure 4B), the symmetry of the capsule should belong to the  $D_{4h}$  point group, and two  $\text{H}^a$  signals should therefore be observed in a 1:2 integral ratio. However, both the  $C_{2v}$ - and the  $D_{4h}$ -symmetric structures are inconsistent with the observation that the signals for the three  $\text{H}^a$  hydrogen atoms appeared in a 1:1:1 integral ratio (Figure 3H). In the final analysis, the NMR spectroscopic data were best explained by the  $D_{2h}$ -symmetric structure, which is formed by distortion of the  $D_{4h}$ -symmetric structure (Figure 4C).<sup>[13]</sup>

The dynamic behavior of  $[\text{Hg}_6\mathbf{1}_8 \cdot \text{A}_{\text{in}} \cdot (\text{TfO}_{\text{in}})_4 \cdot (\text{TfO}_{\text{out}})_6]$  was revealed by 2D exchange spectroscopy (EXSY; Figure 5). The spectrum showed that the three  $\text{H}^a$  hydrogen atoms are chemically exchangeable. The signal  $\text{H}^{aA}$  at  $\delta = 9.03 \text{ ppm}$  was assigned to  $\text{H}^a$  of the pyridine rings coordinated to  $\text{Hg}^{\text{II}}$  bound by a sulfonate group of  $\text{A}^{2-}$ , and the other two signals at around  $\delta = 8.62 \text{ ppm}$ ,  $\text{H}^{aB}$  and  $\text{H}^{aC}$ , were ascribable to  $\text{H}^a$  of the pyridine rings coordinated to  $\text{Hg}^{\text{II}}$  bound by two axial  $\text{TfO}^-$  ligands in light of the similarity of the chemical-shift



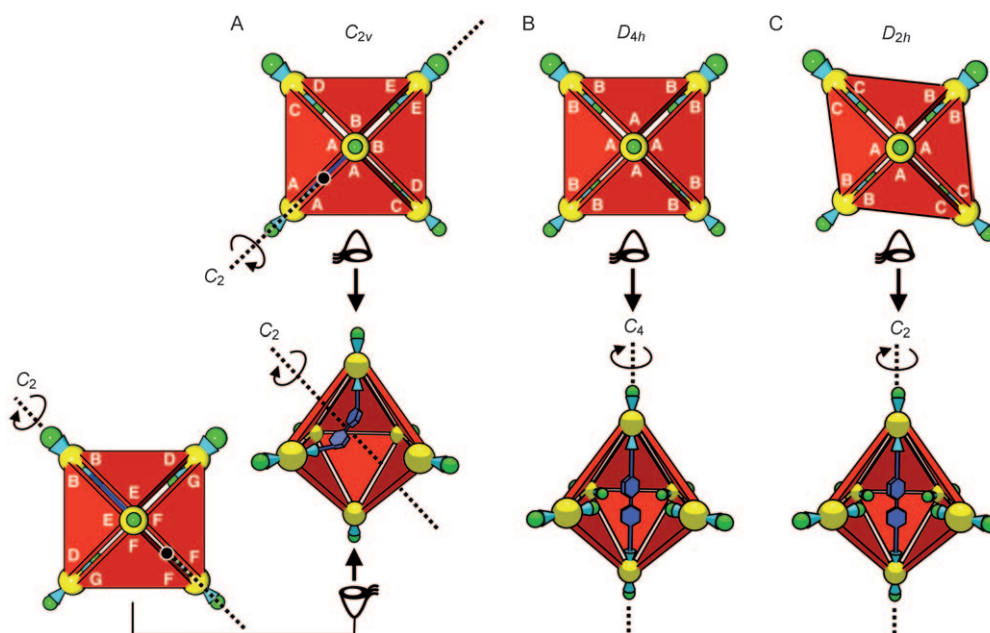


**Figure 4.** Schematic representation of  $[\text{Hg}_6\mathbf{1}_8\cdot\mathbf{A}_{\text{in}}\cdot(\text{TfO}_{\text{in}})_4\cdot(\text{TfO}_{\text{out}})_6]$  capsule complexes. A) A  $C_{2v}$ -symmetric structure with one  $\mathbf{A}^{2-}$  ligand connecting two adjacent  $\text{Hg}^{\text{II}}$  centers; B) a  $D_{4h}$ -symmetric structure with one  $\mathbf{A}^{2-}$  ligand connecting two opposite  $\text{Hg}^{\text{II}}$  vertices; C) a  $D_{2h}$ -symmetric structure with one  $\mathbf{A}^{2-}$  ligand connecting two opposite  $\text{Hg}^{\text{II}}$  vertices; this structure results from distortion of the  $D_{4h}$ -symmetric structure.

values to those observed for  $[\text{Hg}_6\mathbf{1}_8\cdot(\text{TfO}_{\text{in}})_6\cdot(\text{TfO}_{\text{out}})_6]$ . The rates of chemical exchange of these hydrogen atoms,  $k_{(A-B)}$ ,  $k_{(A-C)}$ , and  $k_{(B-C)}$ , were determined to be 0.23, 0.28, and  $1.4\text{ s}^{-1}$ , respectively, from the peak amplitude of these signals, according to a procedure described in the Supporting Information. This result indicates that fast and slow chemical exchange corresponds to structural interconversion in the  $D_{2h}$  capsule and inner-capsule ligand exchange between  $\mathbf{A}_{\text{in}}^{2-}$  and  $\text{TfO}_{\text{in}}^-$ , respectively.

In the  $^{19}\text{F}$  NMR spectrum at 263 K of a solution containing an 8.8:1 mixture of  $[\text{Hg}_6\mathbf{1}_8\cdot\mathbf{A}_{\text{in}}\cdot(\text{TfO}_{\text{in}})_4\cdot(\text{TfO}_{\text{out}})_6]$  and  $[\text{Hg}_6\mathbf{1}_8\cdot(\text{TfO}_{\text{in}})_6\cdot(\text{TfO}_{\text{out}})_6]$ , two signals for  $\text{TfO}_{\text{in}}^-$  were observed at  $\delta = 86.12$  and  $86.17$  ppm in a 3:2 integral ratio. In light of the contribution of  $[\text{Hg}_6\mathbf{1}_8\cdot(\text{TfO}_{\text{in}})_6\cdot(\text{TfO}_{\text{out}})_6]$  to the spectrum, we concluded that the  $[\text{Hg}_6\mathbf{1}_8\cdot\mathbf{A}_{\text{in}}\cdot(\text{TfO}_{\text{in}})_4\cdot(\text{TfO}_{\text{out}})_6]$  capsule showed two chemically nonequivalent  $\text{TfO}_{\text{in}}^-$  signals with the same integral value. The observation of two nonequivalent  $\text{TfO}_{\text{in}}^-$  ligands is ascribable to  $D_{2h}$  symmetry of the  $[\text{Hg}_6\mathbf{1}_8\cdot\mathbf{A}_{\text{in}}\cdot(\text{TfO}_{\text{in}})_4\cdot(\text{TfO}_{\text{out}})_6]$  capsule (Figure 4C). Interestingly, these two different  $\text{TfO}_{\text{in}}^-$  signals became a single broadened signal at 293 K. This result shows that the inner-capsule ligand exchange of the  $\text{TfO}_{\text{in}}^-$  ligands of  $[\text{Hg}_6\mathbf{1}_8\cdot\mathbf{A}_{\text{in}}\cdot(\text{TfO}_{\text{in}})_4\cdot(\text{TfO}_{\text{out}})_6]$  is relatively fast on the NMR timescale at 293 K, whereas the inner-capsule ligand exchange of  $\mathbf{A}_{\text{in}}^{2-}$  with  $\text{TfO}_{\text{in}}^-$  is rather slow on the NMR timescale at the same temperature.

When two  $\mathbf{A}^{2-}$  ligands were incorporated into the capsule, broadened signals were observed in the  $^1\text{H}$  NMR spectrum (Figure 3E), and the  $^{19}\text{F}$  NMR spectrum exhibited two main signals for  $\text{TfO}_{\text{in}}^-$  (Figure 2). These results suggest that further distortion of the capsule takes place as a result of the steric constraint between the two  $\mathbf{A}^{2-}$  ligands in  $[\text{Hg}_6\mathbf{1}_8\cdot(\mathbf{A}_{\text{in}})_2\cdot(\text{TfO}_{\text{in}})_2\cdot(\text{TfO}_{\text{out}})_6]$ . A molecular-modeling study of four possible structural isomers also suggested that a structure in

which two  $\mathbf{A}^{2-}$  ligands bridge two opposite  $\text{Hg}^{\text{II}}$  vertices is more stable than the other three isomers (see Figure S8 in the Supporting Information).

In the two species  $[\text{Hg}_6\mathbf{1}_8\cdot\mathbf{A}_{\text{in}}\cdot(\text{TfO}_{\text{in}})_4\cdot(\text{TfO}_{\text{out}})_6]$  and  $[\text{Hg}_6\mathbf{1}_8\cdot(\mathbf{A}_{\text{in}})_2\cdot(\text{TfO}_{\text{in}})_2\cdot(\text{TfO}_{\text{out}})_6]$ , four and two exchangeable  $\text{TfO}_{\text{in}}^-$  ligands remain inside the capsule, respectively. We next examined further ligand exchange of these remaining  $\text{TfO}_{\text{in}}^-$  ligands with monosulfonate ligands.<sup>[14]</sup> When  $\text{Me}_4\text{NOTs}$  (4 equiv) was added to  $[\text{Hg}_6\mathbf{1}_8\cdot\mathbf{A}_{\text{in}}\cdot(\text{TfO}_{\text{in}})_4\cdot(\text{TfO}_{\text{out}})_6]$ , all four  $\text{TfO}_{\text{in}}^-$  ligands were replaced preferentially with  $\text{TsO}^-$  ligands to form  $[\text{Hg}_6\mathbf{1}_8\cdot\mathbf{A}_{\text{in}}\cdot(\text{TsO}_{\text{in}})_4\cdot(\text{TfO}_{\text{out}})_6]$  (Figure 3F), as demonstrated by  $^1\text{H}$  NMR spectroscopy as well as ESI-TOF mass spectrometry.<sup>[15]</sup> All  $\text{H}^a$  signals of  $[\text{Hg}_6\mathbf{1}_8\cdot\mathbf{A}_{\text{in}}\cdot(\text{TsO}_{\text{in}})_4\cdot(\text{TfO}_{\text{out}})_6]$  were shifted to a lower magnetic field (Figure 3F, I). This result indicates that all  $\text{TfO}_{\text{in}}^-$  ligands were replaced with  $\mathbf{A}^{2-}$  and  $\text{TsO}^-$  and simultaneously pushed out of the capsule, as confirmed by the lack of signals found for  $\text{TfO}_{\text{in}}^-$  in the  $^{19}\text{F}$  NMR spectrum (see Figure S1D in the Supporting Information).<sup>[16]</sup> Unfortunately, most of the  $^1\text{H}$  NMR signals overlapped with one another and did not provide any useful information about the structure. However, in terms of the structural similarity of  $[\text{Hg}_6\mathbf{1}_8\cdot\mathbf{A}_{\text{in}}\cdot(\text{TsO}_{\text{in}})_4\cdot(\text{TfO}_{\text{out}})_6]$  to the  $[\text{Hg}_6\mathbf{1}_8\cdot\mathbf{A}_{\text{in}}\cdot(\text{TfO}_{\text{in}})_4\cdot(\text{TfO}_{\text{out}})_6]$  complex, it is apparent that the bisulfonate  $\mathbf{A}^{2-}$  of the  $[\text{Hg}_6\mathbf{1}_8\cdot\mathbf{A}_{\text{in}}\cdot(\text{TsO}_{\text{in}})_4\cdot(\text{TfO}_{\text{out}})_6]$  capsule bridges two opposite  $\text{Hg}^{2+}$  vertices to reinforce the capsule structure, as supported by the molecular-modeling study (see Figure S8 and Table S2 in the Supporting Information).

In conclusion, one or two rod-shaped bridging bisulfonate ligands  $\mathbf{A}^{2-}$  were successfully incorporated into an octahedral  $\text{Hg}^{\text{II}}$  nanocapsule by the site-selective ligand exchange of inner  $\text{TfO}_{\text{in}}^-$  ligands to form the complexes  $[\text{Hg}_6\mathbf{1}_8\cdot\mathbf{A}_{\text{in}}\cdot(\text{TfO}_{\text{in}})_4\cdot(\text{TfO}_{\text{out}})_6]$  and  $[\text{Hg}_6\mathbf{1}_8\cdot(\mathbf{A}_{\text{in}})_2\cdot(\text{TfO}_{\text{in}})_2\cdot(\text{TfO}_{\text{out}})_6]$ , respectively. The nearly stepwise incorporation of

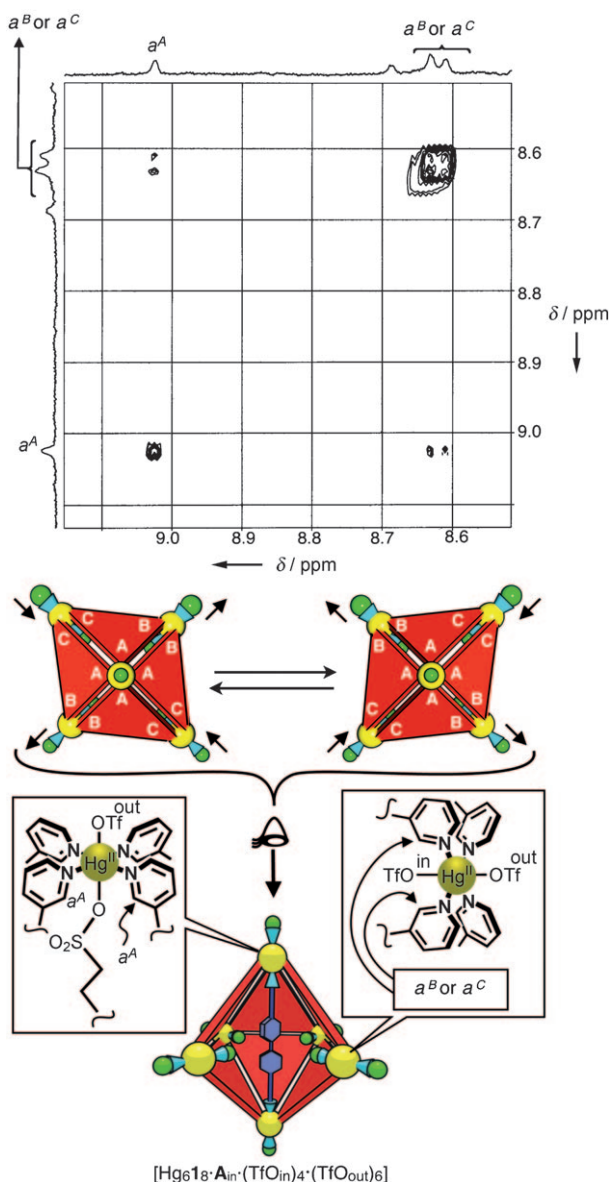


**Figure 5.** Partial 2D EXSY spectrum of  $[\text{Hg}_6\mathbf{18}\cdot\mathbf{A}_{\text{in}}\cdot(\text{TfO}_{\text{in}})_4\cdot(\text{TfO}_{\text{out}})_6]$  (500 MHz,  $\text{CD}_3\text{CN}$ , 293 K, mixing time: 0.7 s).

$\mathbf{A}^{2-}$  was confirmed by ESI-TOF mass spectrometry, and the structure of the  $[\text{Hg}_6\mathbf{18}\cdot\mathbf{A}_{\text{in}}\cdot(\text{TfO}_{\text{in}})_4\cdot(\text{TfO}_{\text{out}})_6]$  capsule was characterized in detail by various NMR spectroscopic experiments. Furthermore, the subsequent ligand exchange of  $\text{TfO}_{\text{in}}^-$  with  $\text{TsO}^-$  inside the capsule produced the complex  $[\text{Hg}_6\mathbf{18}\cdot\mathbf{A}_{\text{in}}\cdot(\text{TsO}_{\text{in}})_4\cdot(\text{TfO}_{\text{out}})_6]$  with two different sulfonate ligands inside. This synthetic strategy based on the use of precisely designed bridging ligands for site-selective ligand exchange has the great advantage that the position of entrapped functional molecule(s) can be controlled. Further investigations on the reactivity of other isostructural metal-capsules, the introduction of functional bridging bisulfonates, and molecular recognition in the spatially well-controlled interior of the capsules are currently underway.

Received: September 29, 2009

Published online: November 26, 2009

**Keywords:** mercury · molecular capsules · self-assembly · sulfonate ligands · supramolecular chemistry

- [1] For examples of covalent organic capsules, see: a) D. J. Cram, *Science* **1983**, 219, 1177; b) D. J. Cram, J. M. Cram, *Container Molecules and their Guests*, Royal Society of Chemistry, Cambridge, UK, **1994**; c) A. Jasat, J. C. Sherman, *Chem. Rev.* **1999**, 99, 931; d) T. Inomata, K. Konishi, *Chem. Commun.* **2003**, 1282; e) X. Liu, Y. Liu, G. Li, R. Warmuth, *Angew. Chem.* **2006**, 118, 915; *Angew. Chem. Int. Ed.* **2006**, 45, 901; f) N. Nishimura, K. Kobayashi, *Angew. Chem.* **2008**, 120, 6351; *Angew. Chem. Int. Ed.* **2008**, 47, 6255; g) K. Srinivasan, B. C. Gibb, *Chem. Commun.* **2008**, 4640; h) V. Steinmetz, F. Couty, O. R. P. David, *Chem. Commun.* **2009**, 343.
- [2] For examples of hydrogen-bonded capsules, see: a) A. Shivan-yuk, J. Rebek, Jr., *Proc. Natl. Acad. Sci. USA* **2001**, 98, 7662; b) J. L. Atwood, L. J. Barbour, A. Jerga, *Proc. Natl. Acad. Sci. USA* **2002**, 99, 4837; c) M. Yamanaka, A. Shivan-yuk, J. Rebek, Jr., *Proc. Natl. Acad. Sci. USA* **2004**, 101, 2669; d) S. Shimizu, T. Kiuchi, N. Pan, *Angew. Chem.* **2007**, 119, 6562; *Angew. Chem. Int. Ed.* **2007**, 46, 6442; e) P. Baillargeon, Y. L. Dory, *J. Am. Chem. Soc.* **2008**, 130, 5640.
- [3] a) M. Tominaga, K. Suzuki, M. Kawano, T. Kusakawa, T. Ozeki, S. Sakamoto, K. Yamaguchi, M. Fujita, *Angew. Chem.* **2004**, 116, 5739; *Angew. Chem. Int. Ed.* **2004**, 43, 5621; b) A. J. Terpin, M. Ziegler, D. W. Johnson, K. N. Raymond, *Angew. Chem.* **2001**, 113, 161; *Angew. Chem. Int. Ed.* **2001**, 40, 157; c) S. P. Argent, H. Adams, T. Riis-Johannessen, J. C. Jeffery, L. P. Harding, M. D. Ward, *J. Am. Chem. Soc.* **2006**, 128, 72; d) B. Olenyuk, J. A. Whiteford, A. Fechtenkötter, P. J. Stang, *Nature* **1999**, 398, 796; e) C. J. Kuehl, Y. K. Kryshchenko, U. Radhakrishnan, S. R. Seidel, S. D. Huang, P. J. Stang, *Proc. Natl. Acad. Sci. USA* **2002**, 99, 4932; f) R. M. McKinlay, G. W. V. Cave, J. L. Atwood, *Proc. Natl. Acad. Sci. USA* **2005**, 102, 5944; g) N. P. Power, S. J. Dalgarno, J. L. Atwood, *Angew. Chem.* **2007**, 119, 8755; *Angew. Chem. Int. Ed.* **2007**, 46, 8601; h) F. Fochi, P. Jacopozzi, E. Wegelius, K. Rissanen, P. Cozzini, E. Marastoni, E. Fiescaro, P. Manini, R. Fokkens, E. Dalcanele, *J. Am. Chem. Soc.* **2001**, 123, 7539; i) C. J. Sumby, M. J. Hardie, *Angew. Chem.* **2005**, 117, 6553; *Angew. Chem. Int. Ed.* **2005**, 44, 6395; j) T. Brasey, R. Scopelliti, K. Severin, *Chem. Commun.* **2006**, 3308; k) D. Moon, S. Kang, J. Park, K. Lee, R. P. John, H. Won, G. H. Seong, Y. S. Kim, G. H. Kim, H. Rhee, M. S. Lah, *J. Am. Chem. Soc.* **2006**, 128, 3530.
- [4] a) S. Hiraoka, T. Yi, M. Shiro, M. Shionoya, *J. Am. Chem. Soc.* **2002**, 124, 14510; b) S. Hiraoka, K. Harano, M. Shiro, M. Shionoya, *Angew. Chem.* **2005**, 117, 2787; *Angew. Chem. Int. Ed.* **2005**, 44, 2727; c) S. Hiraoka, K. Harano, M. Shiro, Y. Ozawa, N. Yasuda, K. Toriumi, M. Shionoya, *Angew. Chem.* **2006**, 118, 6638; *Angew. Chem. Int. Ed.* **2006**, 45, 6488; d) K. Harano, S. Hiraoka, M. Shionoya, *J. Am. Chem. Soc.* **2007**, 129, 5300.
- [5] For examples of self-assembled capsules formed by the hydrophobic effect, see: a) C. L. D. Gibb, B. C. Gibb, *J. Am. Chem. Soc.* **2004**, 126, 11408; b) M. D. Giles, S. Liu, R. L. Emanuel, B. C. Gibb, S. M. Grayson, *J. Am. Chem. Soc.* **2008**, 130, 14430; c) S. Hiraoka, K. Harano, M. Shiro, M. Shionoya, *J. Am. Chem. Soc.* **2008**, 130, 14368; d) S. Hiraoka, K. Harano, T. Nakamura, M. Shiro, M. Shionoya, *Angew. Chem.* **2009**, 121, 7140; *Angew. Chem. Int. Ed.* **2009**, 48, 7006.
- [6] For examples of foldamers with encapsulation properties, see: a) A. Tanatani, M. J. Mio, J. S. Moore, *J. Am. Chem. Soc.* **2001**, 123, 1792; b) C. Bao, B. Kauffmann, Q. Gan, K. Srinivas, H. Jiang, I. Huc, *Angew. Chem.* **2008**, 120, 4221; *Angew. Chem. Int. Ed.* **2008**, 47, 4153.
- [7] For examples of catalysis in self-assembled capsules, see: a) H. Ito, T. Kusakawa, M. Fujita, *Chem. Lett.* **2000**, 598; b) J. Chen, S. Körner, S. L. Craig, D. M. Rudkevich, J. Rebek, Jr., *Nature* **2002**,

- 415, 385; c) D. Fiedler, R. G. Bergman, K. N. Raymond, *Angew. Chem.* **2004**, *116*, 6916; *Angew. Chem. Int. Ed.* **2004**, *43*, 6748; d) M. Yoshizawa, M. Tamura, M. Fujita, *Science* **2006**, *312*, 251; e) M. D. Pluth, R. G. Bergman, K. N. Raymond, *Science* **2007**, *316*, 85.
- [8] For recent examples of the selective functionalization of the inner or outer surfaces of molecular architectures, see: a) J. L. Mynar, T. Yamamoto, A. Kosaka, T. Fukushima, N. Ishii, T. Aida, *J. Am. Chem. Soc.* **2008**, *130*, 1530; b) Y. Goto, H. Sato, S. Shinkai, K. Sada, *J. Am. Chem. Soc.* **2008**, *130*, 14354; c) J. Nakazawa, D. P. Stack, *J. Am. Chem. Soc.* **2008**, *130*, 14360; d) J. D. Henao, Y.-W. Suh, J.-K. Lee, M. C. Kung, H. H. Kung, *J. Am. Chem. Soc.* **2008**, *130*, 16142.
- [9] The inner and outer TfO<sup>−</sup> ligands were assigned by <sup>19</sup>F diffusion-ordered NMR spectroscopy (DOSY; see the Supporting Information).
- [10] In all cases, the quantitative formation of the starting [Hg<sub>6</sub>1<sub>8</sub>·(TfO<sub>in</sub>)<sub>6</sub>·(TfO<sub>out</sub>)<sub>6</sub>] complex was confirmed by <sup>1</sup>H NMR spectroscopy in CD<sub>3</sub>CN prior to ESI-TOF mass measurement.
- [11] In contrast, when the monosulfonate **B**<sup>−</sup>, which has a 4,4'-biphenyldiol moiety similar to that in **A**<sup>2−</sup>, was used, five TfO<sub>in</sub><sup>−</sup> ligands of [Hg<sub>6</sub>1<sub>8</sub>·(TfO<sub>in</sub>)<sub>6</sub>·(TfO<sub>out</sub>)<sub>6</sub>] were replaced with **B**<sup>−</sup> (see Figure S6 in the Supporting Information).
- [12] If **A**<sup>2−</sup> is located outside the capsule, the log *D* value of the hydrogen atoms of **A**<sup>2−</sup> should be larger than that of the capsule structure in light of the observation that the log *D* value of TfO<sub>out</sub><sup>−</sup> is larger than those of both TfO<sub>in</sub><sup>−</sup> and the capsule part as a result of the faster intermolecular ligand exchange of TfO<sub>out</sub><sup>−</sup> ligands.
- [13] A molecular-modeling study suggested that the capsule structure, in which the two opposite Hg<sup>II</sup> vertices are linked by the bridging ligand **A**<sup>2−</sup>, is more stable than the structure in which **A**<sup>2−</sup> bridges two adjacent Hg<sup>II</sup> centers (see Figure S8 and Table S2 in the Supporting Information).
- [14] The ligand-exchange behavior of TfO<sub>in</sub><sup>−</sup> in the capsule containing **A**<sub>in</sub><sup>2−</sup> depends mainly on the electronic nature of monosulfonate ligands and not on their molecular size (see the Supporting Information for details).
- [15] The addition of Me<sub>4</sub>NOTs to [Hg<sub>6</sub>1<sub>8</sub>·(**A**<sub>in</sub>)<sub>2</sub>·(TfO<sub>in</sub>)<sub>2</sub>·(TfO<sub>out</sub>)<sub>6</sub>] also provided [Hg<sub>6</sub>1<sub>8</sub>·**A**<sub>in</sub>·(TsO<sub>in</sub>)<sub>4</sub>·(TfO<sub>out</sub>)<sub>6</sub>] as a result of the exchange of one **A**<sup>2−</sup> ligand and two TfO<sub>in</sub><sup>−</sup> ligands with four TsO<sup>−</sup> ligands. Thus, the same species with two different sulfonate ligands inside the capsule was obtained through two different pathways.
- [16] Upon the addition of Me<sub>4</sub>NOTs to [Hg<sub>6</sub>1<sub>8</sub>·**A**<sub>in</sub>·(TsO<sub>in</sub>)<sub>4</sub>·(TfO<sub>out</sub>)<sub>6</sub>], the inner **A**<sub>in</sub><sup>2−</sup> ligand was replaced by two TsO<sup>−</sup> ligands, and finally [Hg<sub>6</sub>1<sub>8</sub>·(TsO<sub>in</sub>)<sub>6</sub>·(TfO<sub>out</sub>)<sub>6</sub>] was formed.